Heat Mass Transfer (2014) 50:151–159
DOI 10.1007/s00231-013-1228-6

ORIGINAL

Experimental study of heat and mass transfer of a rolling wheel

Yuan Wu · Minggao Wu · Yongheng Zhang · Liangbi Wang

Received: 30 January 2013 / Accepted: 2 September 2013 / Published online: 26 September 2013

Abstract Heat transfer characteristics of a rolling wheel are investigated by using the naphthalene sublimation technique. The local and average Nusselt numbers are obtained. The results reveal that the local and average Nusselt numbers increase with increasing rotating Reynolds number. Under the same rotating Reynolds number they decrease along the radius direction. After comparing with similar available cases reported, it is found that the results are very close to the results of rotating disk in crossflow under the condition that rotating Reynolds number is equal the main flow Reynolds number.

List of symbols

A	Total mass transfer area of the wheel (m^2)
A_1	The mass transfer area on the side surface of the wheel (m^2)
A_2	Mass transfer area on the peripheral face of the wheel (m^2)
D	Mass diffusivity of naphthalene vapor in air (m^2/s)
h_m	Mass transfer coefficient (m/s)
h_{mr}	Local mass transfer coefficient (m/s)
l	Distance between two points on the roiling wheel (m)
n	Exponent (−)
Nu	Nusselt number (−)
Nu_m	Average Nusselt number (−)
Nu_r	Local Nusselt number (−)
Nu_s	Average Nusselt number of the peripheral face of the wheel (−)
P_{atm}	Atmospheric pressure (Pa)
P_{nw}	Saturated naphthalene vapor pressure (Pa)
P_r	Prandtl number (−)
r	Distance from the test point to the center of the wheel (m)
R	Radius of the wheel (m)
R_g	The ideal gas constant of naphthalene vapor (J/mol k)
Re_ω	Rotating Reynolds number (−)
Re_u	Main flow Reynolds number (−)
Sh	Sherwood number (−)
Sh_r	Local Sherwood number (−)
Sc	Schmidt number (−)
T_w	Saturated temperature on naphthalene surface (K)

Greek

ΔM	Naphthalene sublimation weight during a time period (kg)
$\delta(r)$	Naphthalene sublimation height (m)
v	Kinematic viscosity (m^2/s)
ρ_{nw}	Density of saturated naphthalene vapor (kg/m^3)
ρ_s	Density of solid naphthalene (kg/m^3)
τ	Time period of each test running (s)
ω	Angular speed of the test wheel (1/s)

Y. Wu · M. Wu · Y. Zhang · L. Wang (✉)
School of Mechatronic Engineering, Lanzhou Jiaotong University, Lanzhou 730070, Gansu, China
e-mail: lbwang@mail.lzjtu.cn

Y. Wu · M. Wu · Y. Zhang · L. Wang
Key Laboratory of Railway Vehicle Thermal Engineering, Ministry of Education of China, Lanzhou Jiaotong University, Lanzhou 730070, Gansu, China

1 Introduction

Rolling wheel can be encountered in various vehicles, such as tire and the train wheel. Heat is produced by friction of the tire and the wheel when cars and trains are running. Convective heat transfer is the main way for heat transfer

in such cases. If heat cannot be transferred effectively, the heat will increase the temperature of the surface, and it will affect not only the performance of tire and the train wheel, but also the safety of the tire and the train wheel. Thus, convective heat transfer characteristics of rolling wheel is very useful for designing of the tire and the wheel.

Rolling wheel is quite different from the rotating disk or wheel. Convection heat transfer from a rotating disk is also important in the thermal analysis of rotating components of various types of machinery. Many investigations have been carried out for the rotating disk. Trinkl et al. [1] investigated the mean heat transfer coefficient for a rotating disc subjected to forced streams of air with an angle of attack in a range of Reynolds numbers, and obtained the experimental correlations between Nusselt number and Reynolds number. Shevchuk [2] investigated turbulent heat and mass transfer of a rotating disk for Prandtl and Schmidt numbers much larger than unity using an integral method. Through analyzing of the experimental data, Shevchuk [3] got the relationship of average Nusselt number and the Reynolds number in laminar, transition and turbulent flow in the whole disk. He et al. [4] investigated the rotating disk with coupling influence of the wheel rotating speed and air velocity in wind tunnel with the naphthalene sublimation technique. They obtained experimental correlations of Sherwood number with the coupling Reynolds number and correlations of Nusselt number with the coupling Reynolds number. Beg [5], Cho et al. [6], Jong and Seong [7] investigated heat and mass transfer of the rotating disk and flat plate with naphthalene sublimation. Shevchuk et al. [8, 9] investigated the results of an exact solution of a laminar heat transfer problem for a rotating disk with experimental and integral methods. The results are important in different types of rotating machinery. Zhang et al. [10] investigated convection heat transfer coefficient with the naphthalene sublimation principle through the wind tunnel experiments. Ma et al. [11] studied local heat transfer coefficient of a fixed position on a rotating disk with coupling influence of the disk rotating speed and air stream flow velocity with the naphthalene sublimation technique. Cao et al. [12] investigated the heat and mass transfer on air cooling rotating disk in a disk-cap with naphthalene sublimation, and obtained the relationship of local Sherwood number and rotational Reynolds number. Astarita and Cardone [13] investigated a rotating disk with a relatively small centered jet perpendicularly impinging on it, and obtained a new governing similitude parameter and a heat transfer correlation for the Nusselt number at the wheel centre. Saniei and Yan [14], Wiesche [15] and Chen et al. [16] studied convection heat transfer coefficient from a rotating disk with an air jet impinging on it. Soong [17], Christopher and John [18] investigated convection heat transfer coefficient and flow structure from a rotating disk. Cheng and lin [19] investigated unsteady mass transfer in a steady flow field of a laminar forced flow against a rotating disk and obtained numerical results. Wiesche [20] numerically investigated the aerodynamics of a free rotating disk in forced flow field with constant mean velocity parallel to the disk plane and derived the corresponding heat transfer correlations. Latour et al. [21, 22] studied the local convective heat transfer from a disk mounted on a shaft perpendicular to an air crossflow.

Based on the previous review, it is found that although there are many studies of the heat and mass transfer from a rotating disk with both experimental and numerical methods, there are few reports concerning a rolling wheel as shown in Fig. 1. Some investigations have considered the attacked air stream effects on the heat transfer of a rotating disk with the naphthalene sublimation technique. These studies can be classified into two classes: one is rotation wheel, and the other is moving rotation wheel. But these classes do not include the case of rolling wheel. As shown in Fig. 1, the movement of rolling wheel is quite different from a moving rotation wheel. For rolling wheel case, there should at least be a no moving surface on which the wheel rolls. The no moving wall will enforce interaction to the main attack air stream. There is one line on the wheel which contacts with no moving surface and has zero velocity. The characteristics of fluid flow change drastically compared with rotation wheel and moving rotation wheel. Therefore, the convective heat transfer that depends largely on fluid flow characteristics will be quite different from the heat transfer of a rotation wheel or a moving rotation wheel. From this point of view, the available former results of rotation wheel and moving rotation wheel may not be applied directly to a rolling wheel without further investigation. Motivated by this consideration, this paper carried out experimental investigation of heat transfer characteristics of a rolling wheel. The naphthalene sublimation technique is used in the experiment.

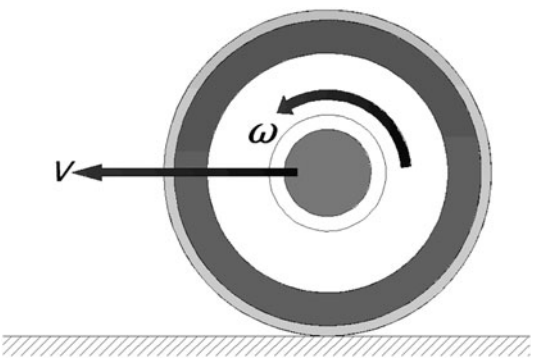

Fig. 1 A rolling wheel with rotating and linear motion

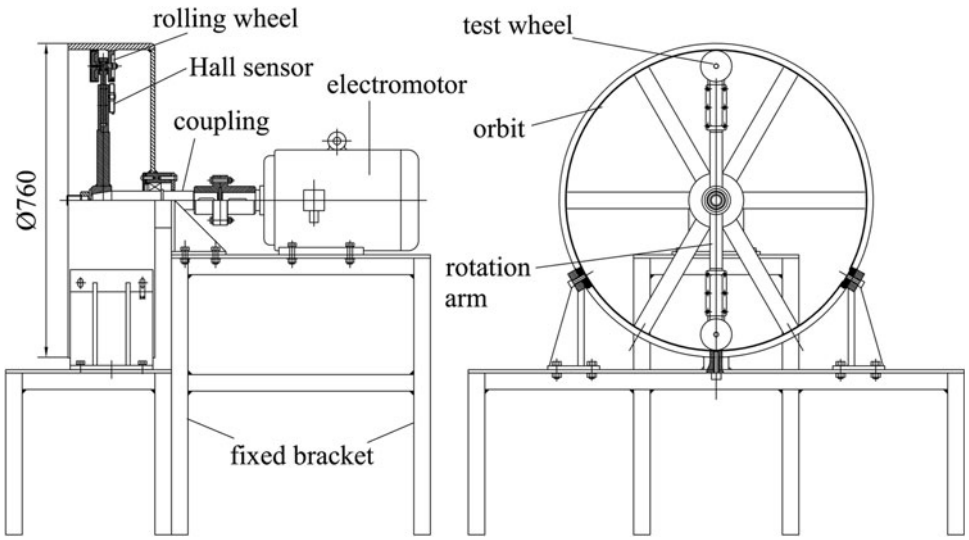

Fig. 2 Schematic view of the experimental apparatus

2 Experimental setup and procedures

To simulate the movement of a rolling wheel, there must have a very long orbit on which the wheel rolls in the laboratory room. However, the laboratory space is limited. In order to establish the movement of rolling wheel and save space, the orbit is designed as a circle shape. Figure 2 shows the schematic diagram of the experimental apparatus. The diameter of the orbit is 760 mm. The rotation arm shafts are made of steel and driven by the electromotor whose speed can be adjusted continuously.

As shown in Fig. 3, the test wheel and rolling wheel are fixed together and have the same rotation speed when rotation arm rotates in the experiment. There is a very small gap (0.5 mm) between the test wheels and the orbit when the rolling wheel is firmly contacted. The part combined by the rolling wheel and test wheel can move in a radial direction when rotation arm rotates. Thus, the contact of the rolling wheel with the orbit relies completely on the centrifugal force. To make sure that the rolling wheel is rolling other than slipping in the experiment, the rotating speed of rolling wheel is measured by Hall sensor that is set close to the rolling wheel and fixed on the end of rotation arm. Another test wheel with the same size is mounted on the rotating wheel in the other end of rotation arm to keep balance. For the purpose of preventing vibration and swing of the experiment apparatus during the experimental process, the fixed bracket is made of steel and is heavy enough in weight. The rotating speed of rolling wheel ranges from 550 to 1,900 r/min.

In order to ensure the weight, the weight of the test wheel should be smaller than the measuring region of electronic balance, thus the test wheel is made of aluminum. Details of test wheel with naphthalene coating are shown in Fig. 4a. The test wheel is shown by slash and the

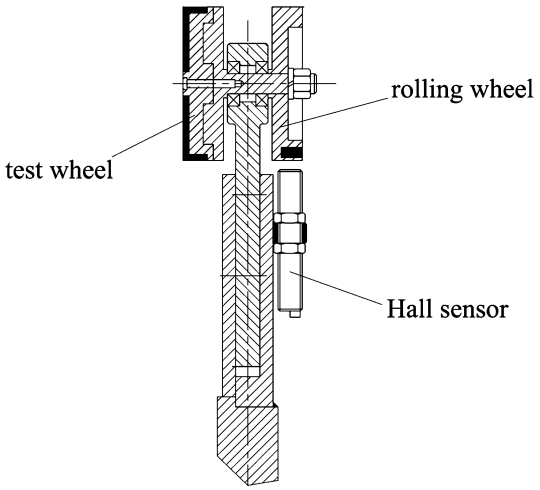

Fig. 3 Schematic view of the test wheel and the rolling wheel

filling indicates the naphthalene. The size of the test wheel is 76 mm in diameter and 15 mm in thickness. The hub used to fix the wheel on the rolling wheel in the center is 12 mm in diameter and 3 mm in thickness, and the diameter of the inner hole is 8 mm. The cast naphthalene is 76 mm in diameter and 3 mm in thickness on the side surface of the test wheel, and the size of cast naphthalene on the peripheral face of the test wheel is 12 mm in height and 3 mm in thickness. There are four lines as shown in Fig. 4b, which are distributed with 90° interval on the side surface of the test wheel to define the measured positions.

There are many available methods to form the naphthalene coating on the test wheel. Goldstein and Cho [23] reviewed and summarized the development of naphthalene sublimation technique and its technical features. Casting is a convenient and effective way. Before casting, the surface of the test wheels and the metallic mold plate must be clean

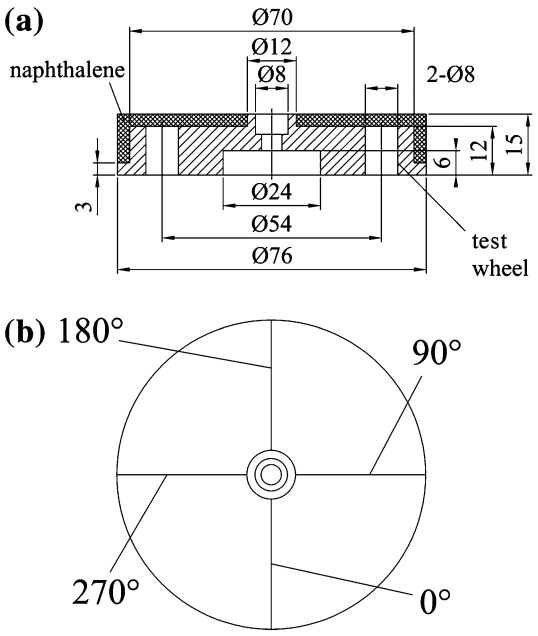

Fig. 4 The test wheel: **a** the test wheel with cast naphthalene; **b** the measure orientation on the test wheel with cast naphthalene

seriously with acetone. The crystal naphthalene is melted in a beaker on an electric stove when heated to about 120 °C, the metallic mold and test wheel are heated to 40 °C. Stop heating when the naphthalene is boiling, cast the molten naphthalene into the test wheels after 30 s. Let the test wheels with molten naphthalene cool naturally in the laboratory room until the naphthalene is completely solidified, then remove the test wheels from the mold and a smooth naphthalene surface can be obtained. Put the test wheels in an airtight glass jar in the laboratory room for 1 day to reach thermal equilibrium in the laboratory room temperature.

After aligning the measurement platform and test wheel by the nicks, the initial height (H_1) of the surface of the test wheel is measured by an inductive micrometer with a capacity of 600 μm and a resolution of 1 μm on the four lines shown in Fig. 4b. The length step along the radius direction is 0.5 mm. As shown in Fig. 4, the line of 0° is the first measuring orientation. Then the test wheel is rotated with 90° clockwise, and sublimation height is measured. Thus, the data on the line of 90° is obtained. The surface heights of remaining two orientations are measured using the same way. The data is recorded on the computer through an A/D converter. The weight of the test wheels is recorded by an electronic balance with a capacity of 250 g and a precision of 0.1 mg. After obtaining the initial weight (M_1) of each test wheel, the test wheels are mounted on the rolling wheels. After running some time, the test wheels are dismounted, then the weight (M_2) of the test wheel and height (H_2) of the surface of the test wheel after sublimation are determined by the way mentioned above. Consequently, the final naphthalene sublimation weight and the surface height of each test wheel can be expressed by the following:

$$\Delta M = M_1 - M_2 \tag{1}$$

$$\delta(r) = H_1 - H_2 \tag{2}$$

Every test wheel can only be used twice in experiment. Thereafter the test wheel cannot be reused and is completely cleaned with acetone prior to recasting. The time period of next four rotating speeds (1,130, 1,410, 1,700, 1,960 r/min) are 4, 3, 3, and 2.5 h, respectively.

3 Experimental principle and data reduction

The naphthalene sublimation technique is an experimental technique employed to determine heat transfer coefficient in convection flow. The basic characteristic of the techniques is that the heat transfer problem to be investigated is replaced by an analogous mass transfer problem. In the laboratory, only mass transfer experiments are performed, and then heat transfer results are obtained by exploring the concept of analogy between heat and mass transfer.

The concept of analogy between heat and mass transfer is based on the fact that for the same geometry and flow condition, Nu and Sh are analogous to each other, and if Pr is equal to Sc, then Nu also equals to Sh.

$$Nu = f(Re, Pr) \quad Sh = f(Re, Sc) \tag{3}$$

In most case, it is very hard to select a fluid having the characteristic that $Pr = Sc$. If air is used as the working fluid, the following relationship exists.

$$Nu = (Pr/Sc)^n Sh \tag{4}$$

where, the exponent n has been found in the range of 1/3 to 0.4, 1/3 is suit for a flat plate in laminar flow, and $Sc = 2.5$ for naphthalene [23–26].

The mass diffusivity of air-naphthalene is obtained from the following expression:

$$D = 0.0681\left(\frac{T_w}{298.13}\right)^{1.93}\left(\frac{101325}{P_{atm}}\right) \tag{5}$$

In Eq. (5), T_w, saturated temperature of naphthalene surface, is equal to the temperature of surroundings, which can be obtained by thermometer. The temperature variation in the diffusivity coefficient is determined from the range of 288–310 K [23–26]. P_{atm} is the local atmosphere pressure.

The average mass transfer coefficient h_m is calculated using the following expressions:

$$h_{\mathrm{m}} = \frac{\Delta M}{\tau A \rho_{\mathrm{nw}}} \tag{6}$$

where τ is the time of the each frequency and A is the mass transfer area of each test wheel, ΔM is the naphthalene sublimation weight of each test wheel, ρ_{nw} is the density of saturated naphthalene vapor at the surface, and is defined by the following law:

$$\rho_{nw} = \frac{P_{nw}}{R_g T_w} \tag{7}$$

where, the ideal gas constant of naphthalene vapor, R_{g}, is equal to 64.87 J/mol/k, P_{nw}, the saturated vapor pressure given from the following expression, is calculated by the expression:

$$\log P_{\mathrm{nw}} = 13.564 - \frac{3729.4}{T_{\mathrm{w}}} \tag{8}$$

The naphthalene vapor prosperities near the solid wall of naphthalene are investigated by many researchers, and the results are summarized by Goldstein [23]. Many investigations indicate that naphthalene vapor near the solid wall of naphthalene can be treated as ideal gas. In Eq. (8), at room temperature, the measuring error of 1 °C will cause the 10 % error of saturated vapor pressure, which will cause the nearly identical error of mass transfer coefficient [26].

After obtaining mass transfer coefficient, Sh can be obtained by

$$Sh = \frac{h_{\mathrm{m}} R}{D} \tag{9}$$

Then, the average Nusselt number can be obtained from Eq. (4) defined by:

$$Nu = (Pr/Sc)^{0.4} Sh \tag{10}$$

The local mass transfer coefficient h_{mr} is defined as:

$$h_{\mathrm{mr}} = \frac{\rho_{\mathrm{s}} \delta(r)}{\rho_{\mathrm{nw}} \tau} \tag{11}$$

where $\delta(r)$ is the naphthalene sublimation height at position r. Again, according to Eq. (8), the local Sh can be obtained by:

$$Sh_{\mathrm{r}} = \frac{h_{\mathrm{mr}} R}{D} \tag{12}$$

The local Nusselt number is:

$$Nu_{\mathrm{r}} = (Pr/Sc)^{0.4} Sh_{\mathrm{r}} \tag{13}$$

The Reynolds number is defined by:

$$Re_{\omega} = \frac{\omega R^2}{v} \tag{14}$$

where ω is the angular speed of the test wheel, R is the radius of the test wheel and v is the kinematics viscosity of air.

The average Nusselt number over total surface A of the test wheel shown in Fig. 5 can be obtained, and the local Nusselt number over surface A_1 can be obtained. In order to obtain the average Nusselt number of surface A_2, following expression is used:

$$\Delta M_{A1} = \Delta M_A - \int_{r_1}^{r_2} 2\pi r \rho_s \delta \mathrm{d}r \tag{15a}$$

$$Nu_{A_1} A_1 = Nu_A A - \int_{r_1}^{r_2} 2\pi r Nu_r \mathrm{d}r \tag{15b}$$

The surface A_1 is divided into sixty unequal annuluses with 0.5 mm in distance.

In the experimental process, the room temperature is kept in a region of 0.1 °C. The uncertainty of temperature, T_{w}, is estimated 0.2 %. The uncertainty of the measured local naphthalene vapor pressure is estimated within 2.5 % according to Eq. (10). The uncertainty of mass diffusivity of air-naphthalene is within 3.5 % according to Eq. (5). The uncertainty of the average mass transfer rate in the present measurement is estimated within 0.6 % according to Eq. (7) with 0.5 % uncertainty in the time period, 0.5 % uncertainty in the area and 0.2 % uncertainty in the mass loss. The maximum uncertainty of the mass transfer coefficient is estimated to be 2.6 % by using Moffat [27] uncertainty estimation method. The uncertainty of local heat transfer coefficient is about 3.5 % according to Eq. (6) with a 0.42 % uncertainty of thermal conductivity of air. The uncertainty of the thermal conductivity is 2 %, so the maximum uncertainty of Nusselt number is <5 % with the same estimation method.

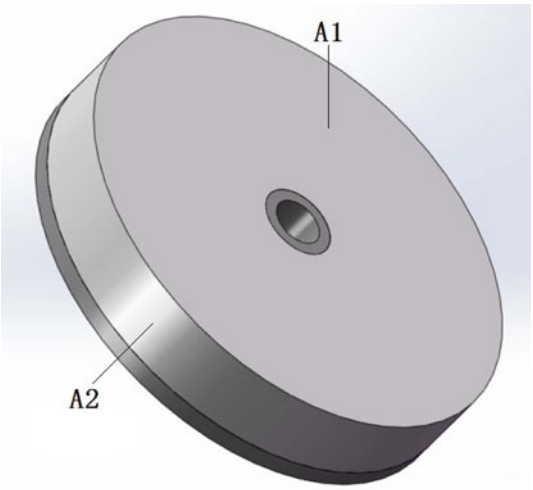

Fig. 5 The mass transfer area of the test wheel

4 Results

In the data reduction process, the Sherwood number has already been transformed into Nusselt number by analogy. Thus, the following discussions are just given to the Nusselt number.

4.1 The local results

The comparison of local Nusselt number getting from the two test wheels with the same Reynolds number is shown in Fig. 6. The A and B represent the different test wheels. It is found that the local Nusselt number is approximately equal with the same Reynolds number. Under the same Re_ω, the Nu_r on the line orientation with 0° has reasonable discrepancy. Because two test wheels have the same configurations and the same moving conditions, thus such results are expected. These results indicate that the repeatability of the experimental results is quite well. Based on the heat transfer performances, two test wheels are quite similar. Therefore, in the following sections, the results getting from one of the test wheel are reported.

The comparison of local Nusselt number on the different orientations under the same rotating Reynolds number is presented in Fig. 7. As shown in Fig. 7, the deviation becomes large with increasing Re_ω. The distribution of observed value is more dispersed when the r/R increase. However, the discrepancy of Nu_r on four measuring lines having different orientations is very small except at small numbers of the points. These results show that under Re_ω region studied, local Nusselt number on the surface of the rolling wheel is independent of the azimuth direction. In this case, local Nusselt number on four measuring lines can be averaged to get local average Nusselt number under the same rotating Reynolds number.

After averaging the local Nusselt number against different orientations, the distribution of the local average Nusselt number along r on the surface of test wheel is shown in Fig. 8. As shown in Fig. 8, Nu_r decreases along the r direction, which is quite surprising. The other information shown in Fig. 8 is that local average Nusselt number increases with increasing Re_ω. There is an obvious position, $r/R = 0.2$, the decreasing slopes of Nu_r changes greatly. When $r/R < 0.2$, Nu_r decreases greatly along the r direction, but when $r/R > 0.2$, Nu_r decreases slowly along the r direction. The reason is not clear now, it is possible that the screw used to fasten the test wheel on the shaft of the rolling wheel will cause some flow distribution.

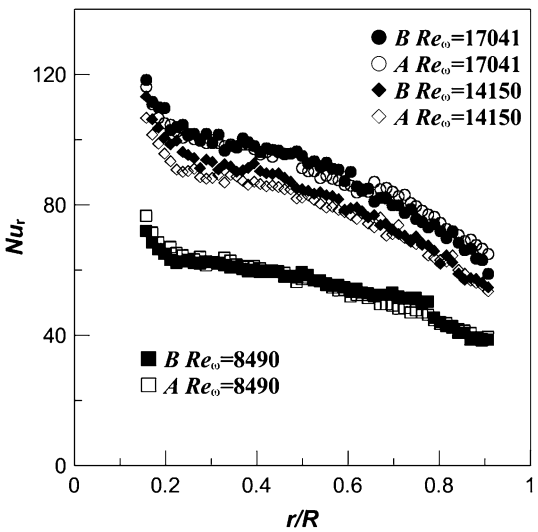

Fig. 6 Comparison of local Nusselt number of the two test wheels on the line having orientation of 0° under the same Reynolds number

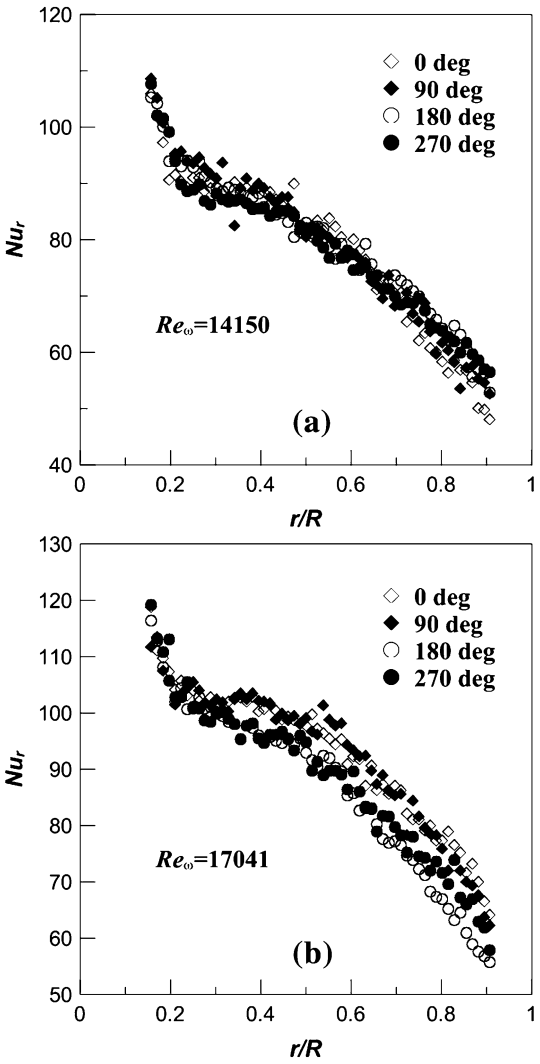

Fig. 7 Comparison of local Nusselt number on four measuring lines having different orientations under the same Reynolds number: **a** $Re_\omega = 14{,}150$, (b) $Re_\omega = 17{,}041$ for Nu_r

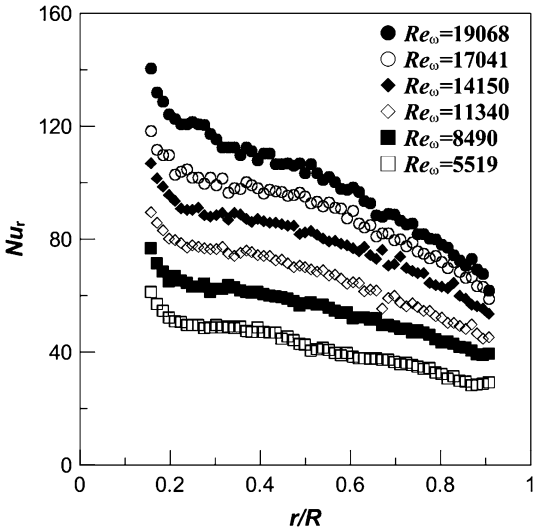

Fig. 8 The distribution of local average Nusselt number along the r direction on the test wheel surface

To explain the results that Nu_r decrease along the r direction, the velocity of a point P on the wheel surface as shown in Fig. 9 should be checked. The time average velocity of P in the time period of one cycle rolling of the wheel can be expressed as:

$$V(r) = \frac{1}{T}\int_0^T \omega l(r,t)\mathrm{d}t \tag{16}$$

In Fig. 9, R is the radius of a circle, l is the distance between point P and Q (contacting point of the wheel on obit), and OP $= r$, T is the time of the wheel rolls a circle; ω is the angular velocity of circle.

The average velocity of the centre of the wheel is constant, which is equal to ωR. The ratio of the average velocity of the point P over the average velocity of the centre is shown in Fig. 10. It is found that the ratio decreases along the r direction. It implies that the average

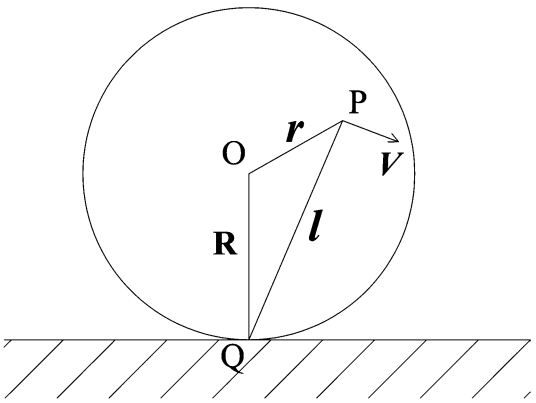

Fig. 9 The velocity of the point P on the wheel

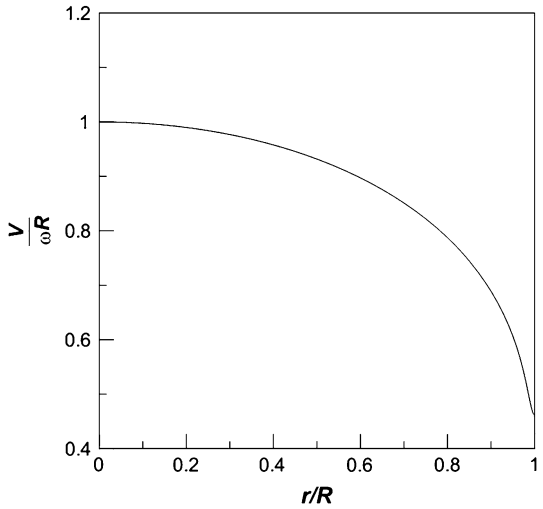

Fig. 10 The ratio of the time average velocity of the point P over the average velocity of the centre versus r/R

velocity of the point P decrease along the r direction. Considering that the fluid flow is the main fact affects the convection heat transfer, Nu_r should decrease along the r direction as the experimental results shown.

4.2 The average results

The average Nusselt number of the test wheel as a function of the rotating Reynolds number is described in Fig. 11. The test wheels run at six different rotating speeds of 550, 845, 1,130, 1,410, 1,700, 1,960 r/min for different time periods. The average results obtained from different experiments and the different test wheel are similar, and the maximum difference between the average results is about 11 % under $Re_\omega = 19{,}068$. It is found that the effect of rotating speed on the Nusselt number is obvious: with

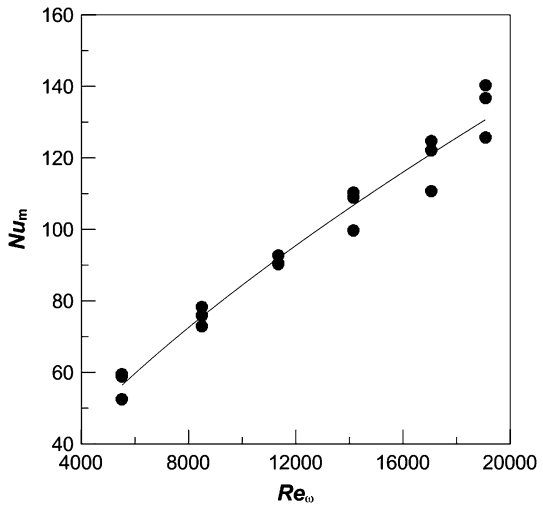

Fig. 11 The average Nusselt number as a function of Re_ω

increasing Re_ω, Nu_m increases. The correlation of the average Nusselt number and average rotating Reynolds number is:

$$Nu_m = 0.166 Re_\omega^{0.676} \quad (17)$$

The average Nusselt number as a function of rotating Reynolds number in the peripheral face of the test wheel is shown in Fig. 12. It is found that with increasing Re_ω, Nu_m increases. By comparing the data shown in Figs. 11 and 12, it is found that the average Nusselt number in the peripheral face of the test wheel is larger than the average Nusselt number of the test wheel. The reason that causes such phenomena is not clear now, and it needs further investigation.

5 Discussion

Wiesche et al. [1, 15, 20] and Latour et al. [21, 22] have reported the relevant works. They investigated heat transfer on the surface of rotating disk with respect to stationary disk in crossflow, rotating disk in still air and rotating disk in crossflow. By dimensional analysis, the mean Nusselt number at steady state can be expressed as,

$$Nu_m = f(Pr, Re_u, Re_\omega) \quad (18)$$

Re_u is defined as

$$Re_u = \frac{u_{in} R}{v} \quad (19)$$

Based on the LES study [15], the correlations of mean Nusselt numbers with Reynolds were obtained and supported by similar studies [21, 22] with reasonable deviation. The heat transfer phenomenon from rolling disk concerned in the present study is very near to the case of

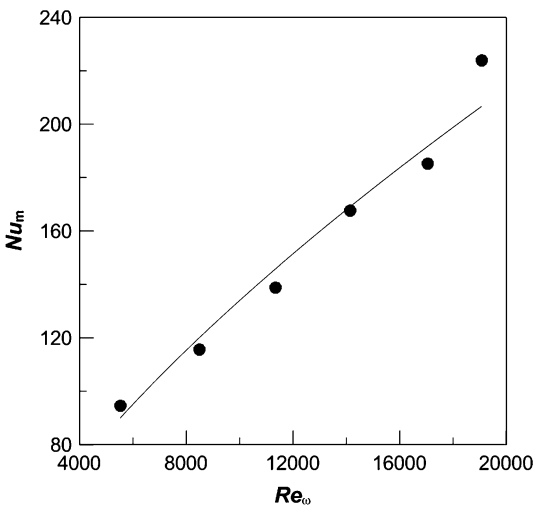

Fig. 12 The average Nusselt number as a function of Re_ω on the peripheral face of the test wheel

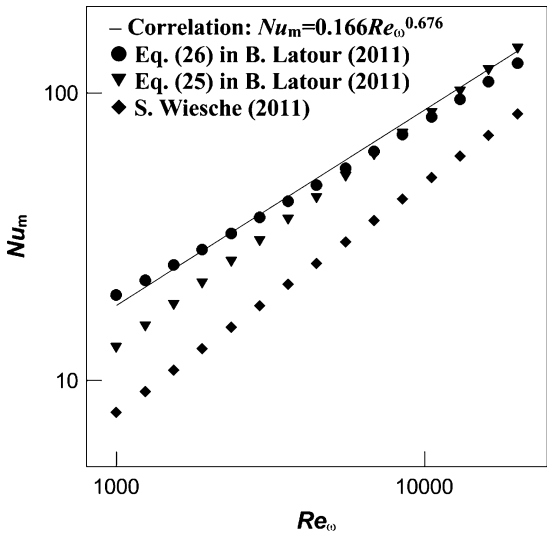

Fig. 13 Comparison between mean Nusselt number of present work and corresponding results

rotating disk in crossflow under the condition that $Re_u = Re_\omega$. The comparison of mean Nusselt number in the present work with the results from literatures [1, 21] is shown in Fig. 13.

It is observed that the correlation of mean Nusselt number against crossflow Reynolds number in the present study has the same trend with others. The correlation of our results are basically in accordance with the results of Latour et al. [21] with a differences of 4.12 % compared with Eq. (25) [21] and 9.08 % compared with Eq. (26) [21] for $Re_u = 12{,}000$. Comparing to the mean Nusselt number of Trinkl's study [21], our result is 43.02 % higher for $Re_u = 12{,}000$. As the presence of shaft in the configuration of the rolling wheel, the mean Nusselt number is greater than the case of crossflow passing over plane rotating disk [1, 15, 20]. This is also confirmed by Latour [21, 22].

In present configuration, the diameter ratio $d/D = 1/10$, but for straight track $d/D = 1/\infty$. Thus, the dimensions of the orbit and the wheels used are not enough to say the dimension effect is negligible. It needs further investigation. After comparing the results from the similar case (rotating disk in crossflow at the condition of $Re_u = Re_\omega$) [21] with our results, it is found that the difference is less than 10 % when $Re_u = 12{,}000$. This indicates the dimension effect may not be large.

6 Conclusions

Local and average heat transfer characteristics on the surface of the test wheel rolling on an orbit are investigated by using naphthalene sublimation technique. The results are expressed by means of local Nusselt number as a function

of *r/R* and average Nusselt number as a function of the Reynolds number. The following conclusions can be drawn:

1. Nusselt number of rolling wheel is very close to the Nusselt number of rotating disk in crossflow with condition that $Re_u = Re_\omega$.
2. The local and average Nusselt numbers on the surface of the rolling wheel increases with increasing rotating Reynolds number.
3. Under the same rotating Reynolds number, local Nusselt number decreases along the *r* direction. The reason is that in one rolling cycle the average velocity on the wheel surface decreases along the *r* direction.

Acknowledgments This work is supported by the National Nature Science Foundation of China (No. 51236003).

References

1. Trinkl CM, Bardas U, Weyck A, Wiesche S (2011) Experimental study of the convective heat transfer from a rotating disc subjected to forced air streams. Int J Therm Sci 50:73–80
2. Shevchuk IV (2009) Turbulent heat and mass transfer over a rotating disk for the Prandtl or Schmidt numbers much larger than unity: an integral method. Heat Mass Transf 45:1313–1321
3. Shevchuk IV (2008) A new evaluation method for Nusselt numbers in naphthalene sublimation experiments in rotating-disk systems. Heat Mass Transf 44:1409–1415
4. He Y, Ma LX, Huang SY (2005) Convection heat and mass transfer from a disk. Heat Mass Transf 41:766–772
5. Beg SA (1973) Forced Convective mass transfer from circular disks. Heat Mass Transf 1:45–51
6. Cho HH, Won CH, Ryu GY, Rhee DH (2003) Local heat transfer characteristics in a single rotating disk and co-rotating disks. Microsyst Technol 9:399–408
7. Jong HP, Seong YY (2004) A naphthalene sublimation study on heat/mass transfer for flow over a flat plate. KSME Int J 18:1258–1266
8. Shevchuk IV (2002) An exact solution for heat transfer of a jet co-axially impinging on a rotating disk and its comparisons with stagnation point experiments. J Therm Sci 11:53–59
9. Shevchuk IV, Buschmann MH (2005) Rotating disk heat transfer in a fluid swirling as a forced vortex. Heat Mass Transf 41: 1112–1121
10. Zhang HH, Wang YZ, Tao WQ (1985) Investigation of forced convective heat transfer using naphthalene sublimation technique. J Eng Thermophys 6:49–55
11. Ma LX, Wang LH, Li QL, Huang SY (2003) Experimental research of convective heat transfer on a disk with coupling of linear movement and rotating. In: Chinese Society of Heat and Mass Transfer (ed) Proceeding of engineering heat thermophysics conference, Beijing, pp 232–238
12. Cao YZ, Lin YZ, Feng HZ, Xu GQ, Qiu XG (1993) Simulative experimental study of heat and mass transfer in rotating disk cooled by air. J Aerosp Power 8:283–287
13. Astarita T, Cardone G (2008) Convective heat transfer on a rotating disk with a centred impinging round je. Int J Heat Mass Transf 51:1562–1572
14. Saniei N, Yan XJ (2000) An experimental study of heat transfer from a disk rotating in an infinite environment including heat transfer enhancement by jet impingement cooling. J Enhanc Heat Transf 7:231–245
15. Wiesche S (2007) Heat transfer from a rotating disk in a parallel air crossflow. Int J Therm Sci 46:745–754
16. Chen YM, Lee WT, Wu SJ (1998) Heat (mass) transfer between an impinging jet and a rotating disk. Heat Mass Transf 34: 195–201
17. Soong CY (2003) Flow structure and heat transfer between two disks rotating independently. J Therm Sci 12:62–76
18. Christopher JE, John KE (2000) Turbulent heat and momentum transport on a rotating disk. J Fluid Mech 402:225–253
19. Cheng WT, Lin HT (1994) Unsteady and steady mass transfer by laminar forced flow against a rotating disk. Heat Mass Transf 30:l01–108
20. Wiesche S (2002) Heat transfer and thermal behavior of a rotating disk passed by a planar air stream. Forsch Ingenieurwes 67:161–174
21. Latour B, Bouvier P, Harmand S (2011) Convective heat transfer on a rotating disk with transverse air crossflow. J Heat Transf 133:021702-1-10
22. Latour B, Harmand S (2012) Local convective heat transfer identification by infrared thermography from a disk mounted on a cylinder in air crossflow. In: 11th international conference on quantitative infrared thermography, Naples, Italy, QIRT2012-106
23. Goldstein RJ, Cho HH (1995) A review of mass transfer measurements using naphthalene sublimation. Exp Therm Fluid Sci 10:416–434
24. Kreith F, Taylor J, Chong JP (1959) Heat and mass transfer from a rotating disk. J Heat Transf 81:95–105
25. Kreith F, Doughman E, Koztowski H (1963) Mass and heat transfer from an enclosed rotating disk with and without source flow. J Heat Transf 85:153–162
26. Cao YZ, Qiu XG (1998) Experimental heat transfer. National Defence Industry Press, Beijing, pp 150–194
27. Moffat RJ (1982) Contributions to the theory of single-sample uncertainty analysis. J Fluids Eng 104:250–258